Fluorescent Supramolecular Polymers: Metal Directed Self-Assembly of Perylene Bisimide Building Blocks

Rainer Dobrawa,[†] Marina Lysetska,[†] Pablo Ballester,[‡] Matthias Grüne,[†] and Frank Würthner*,[†]

Institut für Organische Chemie, Universität Würzburg, Am Hubland, D-97074 Würzburg, Germany, and Institució Catalana de Recerca i Estudis Avançats (ICREA) and Institut Català d'Investigació Química (ICIQ), Avgda. Països Catalans, s/n, 43007-Tarragona, Spain

Received November 3, 2004; Revised Manuscript Received December 2, 2004

ABSTRACT: Complexation properties of 2,2′:6′,2″-terpyridine (tpy) have been studied with a series of first row transition metal ions by UV−vis, ^{1}H NMR, and isothermal titration calorimetry, and ΔH values for the tpy complexation processes have been determined. These studies reveal that terpyridine−Zn^{2+} complex constitutes an ideal supramolecular building block characterized by thermodynamically stable and kinetically labile coordination bonding. Thus, at room-temperature, perylene bisimide fluorophores equipped with one or two terpyridine functionalities formed coordination dimers and polymers, respectively, upon addition of Zn^{2+} metal ions. The reversible formation of coordination dimers and polymers has been established by ^{1}H NMR and additionally by DOSY NMR and fluorescence anisotropy measurements. The optical properties of dimeric and polymeric complexes have been investigated by UV−vis and fluorescence spectroscopy which prove that the Zn^{2+} coordination to the terpyridine unit does not effect the advantageous fluorescence properties of perylene bisimide moieties. Coordination polymer strands can be visualized by atomic force microscopy (AFM), which also reveals the formation of a monolayer film at higher concentration. The average polymer length has been determined by AFM to 15 repeat units, which correlates well with the value estimated by ^{1}H NMR to >10 repeat units.

Introduction

Photoactive organic compounds have gained significant attention in the past decade as materials for organic light emitting diodes (OLEDs)[1] and plastic solar cells.[2] For both applications, photoactive polymers, as well as small-size functional molecules, have been successfully applied.[3] In most cases, device fabrication involves either the spin-coating of soluble polymers or the vacuum deposition of thin films of functional molecules. Although both procedures are meanwhile established, they have certain disadvantages. Polymeric materials are difficult to purify after the polymerization step, and defective linkages disrupting the conjugation cannot be always avoided. Furthermore, solubility of conjugated polymers is often low, thus sophisticated soluble precursor polymers are necessary to make them processable. On the other hand, the vacuum deposition process requires extensive instrumentation, and grain boundaries have detrimental effect on the device properties. The programmed supramolecular organization ("self-assembly") of photoactive components might open a new avenue to overcome these obstacles since small-size molecules are accessible in high purity and their supramolecular polymerization can be accomplished at room temperature in a reversible and predictable manner.

Metal−ligand coordination seems to be particularly attractive for this goal, as it combines defined, directed interactions with high binding constants. In particular, by proper choice of a metal−ligand combination, it is possible to realize ideal conditions for self-assembly, i.e., formation of kinetically labile but nevertheless thermodynamically stable bonds. Accordingly, it is not surprising that metal−ligand coordination polymers, which are processable in solution, have gained considerable interest in the past years.[4−6] The properties of coordination polymers can be widely varied due to the availability of a multitude of metal ions and ligands, both having effect on binding strength, reversibility, and solubility. A ligand which has been of particular importance for the construction of metallosupramolecular systems is 2,2′:6′,2″-terpyridine (tpy). In contrast to the related 2,2′-bipyridine (bpy) ligand, which gives rise to the formation of $M(bpy)_3^{2+}$-type metal complexes with Δ/Λ chirality, tpy forms defined octahedral coordination compounds $M(tpy)_2^{2+}$ with a large number of transition metal ions. Constable and Cargill Thompson have drawn attention to this advantage and have developed the concept for the utilization of ditopic tpy ligands as building blocks for coordination oligomers and polymers.[7] In the past years, a large number of studies has been reported on the construction of linear rods[8−10] and dendrimers[11] using the tpy complexes of kinetically inert Ru^{2+} and Os^{2+} as photochemically active units and examples of coordination polymers built up from tpy ligands have been introduced by several research groups.[12−14]

Although a large number of coordination polymer structures have been reported, only few examples are known where functional units such as dyes have been incorporated into supramolecular coordination polymers.[15−18] Recently, photoactive and mechanoresponsive gels based on tpy-related bis(2,6-bis(1′-methylbenzimidazolyl)-pyridine coordination polymers have been successfully prepared by Beck and Rowan.[19] The adaptability of these materials arises from labile bonding of the ligand to the metal ion, a feature which is not given by classical covalent chemical bonds.

* Author to whom correspondence should be addressed. E-mail: wuerthner@chemie.uni-wuerzburg.de.
† Institut für Organische Chemie.
‡ Institució Catalana de Recerca i Estudis Avançats and Institut Català d'Investigació Química.

10.1021/ma047737j CCC: $30.25
Published on Web 01/25/2005

In the past, perylene bisimide dyes, which exhibit outstanding fluorescence and redox properties, have been applied to construct numerous supramolecular assemblies[20] by $\pi-\pi$-stacking,[21] hydrogen-bonding,[22,23] and metal−ligand interaction.[24,25] Moreover, they have been incorporated in classical polyimide main chain polymers by the groups of Müllen and Thelakkat.[26] Here, we report on metal-directed self-assembly of highly fluorescent perylene bisimides equipped with the 2,2′:6′,2″-terpyridine complexing unit[27] to photoactive coordination polymers and present their spectroscopic and structural properties. In particular, we will show that coordination to Zn^{2+} ions provides an ideal supramolecular bond which combines high thermodynamic stability with fast exchange kinetics and no detrimental effects on the photoluminescence of the perylene bisimide fluorophore.

Experimental Section

General. Solvents were purified and dried according to standard procedures.[28] Chromatography was performed with silica gel 60 (0.035−0.070 mm) and basic alumina, which was deactivated with 4 wt% of water. 4′-*p*-Aminophenyl-2,2′:6′,2″-terpyridine (**2**) was prepared from 4′-*p*-nitrophenyl-2,2′:6′,2″-terpyridine[29] by reduction with Pd/C and hydrazine hydrate in ethanol. Perylene bisanhydrides applied in this work are accessible by literature procedures.[22,24,26] 2,2′:6′,2″-Terpyridine, zinc trifluoromethane sulfonate (triflate, OTf) and the metal perchlorate hexahydrate salts were commercially available. ^{1}H NMR spectra were recorded on a 400 MHz spectrometer and chemical shifts δ (ppm) calibrated against tetramethylsilane (TMS) as internal standard. MALDI-TOF-MS were measured using reflector mode. All fluorescence spectra were corrected. Fluorescence quantum yields were determined by the optical dilute method[30] ($A < 0.05$) using *N*,*N*′-di(2,6-diisopropylphenyl)-1,6,7,12-tetraphenoxyperylene-3,4:9,10-tetracarboxylic acid bisimide ($\Phi_{fl} = 0.96$ in chloroform)[31] as standard. Fluorescence lifetimes were determined by using a 337 nm nitrogen laser/dye laser system. Fluorescence decay curves were evaluated with the software supplied with the instrument. Fluorescence anisotropy measurements were performed employing Glan−Thompson polarizers. Spectroscopy grade solvents were used for UV−vis and fluorescence studies. Details on DOSY NMR, fluorescence anisotropy titrations, isothermal titration calorimetry (ITC), and AFM measurements are given in the Supporting Information.

***t*-Butylphenoxy Ligand 3a.** 1,6,7,12-Tetra(4-*tert*-butylphenoxy)perylene-3,4:6,10-tetracarboxylic acid bisanhydride (**1a**)(0.70 g, 0.71 mmol) was reacted with 4′-*p*-aminophenyl-2,2′:6′,2″-terpyridine (**2**) (0.58 g, 1.79 mmol) and anhydrous zinc acetate as catalyst (70 mg) in quinoline (20 mL) for 5 h at 180 °C under argon. After being cooled to room temperature, the mixture was poured on aqueous HCl (200 mL, 1 M); the resulting precipitate was allowed to settle overnight and isolated by filtration and subsequently washed with water and methanol. The crude product was redissolved in a minimum amount of dichloromethane and precipitated by addition of methanol. Purification was achieved by repetitive column chromatography on aluminum oxide (basic, activity II) with a gradient from $CHCl_3$ to $CHCl_3$/MeOH (90:10) to yield **3a** (415 mg, 37%) as a dark-blue microcrystalline powder. mp > 350 °C; ^{1}H NMR (400 MHz, $CDCl_3$, TMS): δ = 8.78 (s, 4H; H3′, H5′), 8.73 (ddd, J = 5.0, 2.0, 1.0 Hz, 4H; H6, H6″), 8.67 (d, J = 8.0 Hz, 4H; H3, H3″), 8.29 (s, 4H; H_{Pery}), 8.05 (d, J = 8.5 Hz, 4H; H_{Ar}), 7.87 (td, J = 8.0, 2.0 Hz, 4H; H4, H4″), 7.42 (d, J = 8.5 Hz, 4H; H_{Ar}), 7.35 (m, 4H; H5, H5″), 7.24 (d, J = 9.0 Hz, 4H; H_{Ar}), 6.87 (d, J = 9.0 Hz, 4H; H_{Ar}), 1.27 (s, 36H; CH_3); UV−vis ($CHCl_3$): λ_{max} (ϵ) = 590 (54 500), 549 (32 800), 458 nm (17 500 M^{-1} cm^{-1}); fluorescence ($CHCl_3$): λ_{max} = 620 nm, quantum yield ($CHCl_3$): Φ_{fl} = 0.91, lifetime (λ_{ex} = 520 nm, λ_{em} = 645 nm): τ = 6.1 ns ($CHCl_3$), 4.8 ns (DMF); MS (MALDI-TOF, dithranol[32]): *m/z* 1597.51 $[M + H]^+$ (calcd for $C_{106}H_{84}N_8O_8$: 1596.64); elemental analysis calcd (%) for $C_{106}H_{84}N_8O_8$ (1597.9): C 79.68, H 5.30, N 7.01; found C 79.48; H 5.31, N 6.96.

***t*-Octylphenoxy Ligand 3b.** This compound was synthesized and purified in the same way as that described for **3a** starting from the respective 1,6,7,12-tetra(4−1,1,3,3-tetramethylbutylphenoxy)perylene-3,4:6,10-tetracarboxylic acid bisanhydride (**1b**) (400 mg, 0.33 mmol) and 4′-*p*-aminophenyl-2,2′:6′,2″-terpyridine (**2**) (320 mg, 1 mmol) to yield **3b** (72.3 mg, 0.04 mmol, 12%) as a bright-red powder: mp > 350 °C; ^{1}H NMR (400 MHz, $CDCl_3$, TMS): δ = 8.78 (s, 4H; H3′, H5′), 8.72 (d, J = 4.0 Hz, 4H; H6, H6″), 8.66 (d, J = 8.0 Hz, 4H; H3, H3″), 8.22 (s, 4H; H_{Pery}), 8.03 (d, J = 8.5 Hz, 4H; H3‴, H5‴), 7.86 (td, J = 7.5, 2.0 Hz, 4H; H4, H4″), 7.40 (d, 2H, J = 5.5 Hz, 4H; H2‴, H6‴), 7.35 (dd, J = 7.0, 5.0 Hz, 4H; H5, H5″), 7.17 (d, J = 8.5 Hz, 8H; H_{Ar}), 6.85 (d, J = 8.5 Hz, 8H; H_{Ar}), 1.71 (s, 8H; CH_2), 1.34 (s, 24H; CH_3); 0.75 (s, 36H; CH_3); UV−vis (CH_2Cl_2): λ_{max} (ϵ) = 586 (54 800), 548 (33 800), 453 nm (18 100 M^{-1} cm^{-1}); fluorescence (CH_2Cl_2): λ_{max} = 620 nm, quantum yield (CH_2Cl_2): Φ_{fl} = 0.95; MS (MALDI-TOF, DHB[32]): *m/z* 1821.74 $[M + H]^+$ (calcd for $C_{122}H_{116}N_8O_8$: 1820.89); elemental analysis calcd (%) for $C_{122}H_{116}N_8O_8 \cdot H_2O$ (1840.3): C 79.62, H 6.46, N 6.09; found: C 79.89, H 6.42, N 5.94.

Monotopic Ligands 5a,b. The respective mixtures[24] of mono- (**4a,b**) and bisanhydrides (**1a,b**) (contains 20% of monoanhydride) were reacted with 4′-*p*-aminophenyl-2,2′:6′,2″-terpyridine (**2**) and purified accordingly, as described above. Monotopic *tert*-butylphenoxy ligand **5a** (353 mg, 0.26 mmol, 40% referred to the amount of monoanhydride), blue powder: mp > 350 °C; ^{1}H NMR (400 MHz, $CDCl_3$, TMS): δ = 8.76 (s, 2H; H3′, H5′), 8.72 (ddd, J = 5.0, 2.0, 1.0 Hz, 2H; H6, H6′), 8.66 (dt, J((H,H) = 8.0, 1.0 Hz, 2H; H3, H3′), 8.26 (s, 2H; H_{Pery}), 8.25 (s, 2H; H_{Pery}), 8.04 (d, J = 8.5 Hz, 2H; H_{Ar}), 7.87 (td, J = 7.5, 2.0 Hz, 2H; H4, H4′), 7.41 (d, J = 8.5 Hz, 2H; H_{Ar}), 7.35 (m, 2H; H5, H5′), 7.26−7.22 + $CHCl_3$ (m; H_{Ar}), 7.87−6.83 (m, 8H; H_{Ar}), 4.12 (t, J = 7.5 Hz, 2H; NCH_2), 1.67 (m, 2H; CH_2), 1,43 (m, 2H; CH_2), 1.30 (s, 18H; CH_3), 1.26 (s, 18H; CH_3), 0.94 (t, J = 7.5 Hz, 3H; CH_3); UV−vis ($CHCl_3$): λ_{max} (ϵ) = 587 (52 100), 547 (31 000), 455 nm (17 700 M^{-1} cm^{-1}); fluorescence ($CHCl_3$): λ_{em} = 622 nm, quantum yield ($CHCl_3$): Φ_{fl} = 0.89; MS (MALDI-TOF, dithranol): *m/z* 1346.50 $[M + H]^+$ (calcd for $C_{89}H_{79}N_5O_8$: 1345.59); elemental analysis calcd (%) for $C_{89}H_{79}N_5O_8$ (1346.61): C 79.38, H 5.91, N 5.20; found C 79.18; H 6.08, N 5.12. Monotopic *tert*-octylphenoxy ligand **5b**: (10 mg, 0.06 mmol, 7% referred to the amount of monoanhydride), bright-red powder: mp > 350 °C; ^{1}H NMR (400 MHz, $CDCl_3$, TMS): δ = 8.77 (s, 2H; H3′, H5′), 8.72 (d, J = 4.0 Hz, 2H; H6, H6″), 8.66 (d, J = 8.0 Hz, 2H; H3, H3″), 8.19 (s, 2H; H_{Pery}), 8.18 (s, 2H; H_{Pery}), 8.03 (d, J = 8.5 Hz, 2H; H3‴, H5‴), 7.86 (td, J = 7.5, 2.0 Hz, 2H; H4, H4″), 7.40 (d, 2H, J = 5.5 Hz, 2H; H2‴, H6‴), 7.35 (dd, J = 7.0, 5.0 Hz, 2H; H5, H5″), 7.29−7.25 (m, 8H; H_{Ar}), 6.89−6.85 (m, 8H; H_{Ar}), 4.11 (t, J = 7.5 Hz, 2H; NCH_2), 1.73 (s, 4H; CH_2), 1.70 (s, 4H; CH_2), 1.65 (m, 2H; CH_2); 1.43−1.33 (m, 26H; CH_3), 0.94 (t, J = 7.0 Hz, 3H; CH_3), 0.79 (s, 18H; CH_3), 0.75 (s, 18H; CH_3); UV−vis ($CHCl_3$): λ_{max} (ϵ) = 590 (49 000), 549 (29 400), 454 nm (17 500 M^{-1} cm^{-1}); fluorescence ($CHCl_3$): λ_{max} = 620 nm, quantum yield ($CHCl_3$): Φ_{fl} = 0.90; MS (MALDI-TOF, dithranol): *m/z* 1570.58 $[M + H]^+$ (calcd for $C_{105}H_{111}N_5O_8$: 1569.84); elemental analysis calcd (%) for $C_{105}H_{111}N_5O_8$ (1571.0): C 80.27, H 7.12, N 4.46; found: C 79.72, H 7.13, N 4.24.

Complex 6a. To a solution of the monotopic ligand **5a** (13.3 mg, 9.8 μmol) in $CHCl_3-CH_3CN$ (80:20, 4 mL) a stock solution of zinc triflate (10 mM, 490 μL, 4.9 μmol) was added and the solution was stirred for 1 h at room temperature. Exact 2:1 stoichiometry is confirmed by ^{1}H NMR and, if necessary, is adjusted until no residual signals of the uncomplexed ligand is present. The solution was concentrated; the product was precipitated by addition of more acetonitrile (10 mL) and isolated quantitatively by centrifugation. ^{1}H NMR (400 MHz, $CDCl_3/CD_3CN$ (80:20), TMS): δ = 9.00 (s, 4H; H3′, H5′), 8.72 (d, J = 8.5 Hz, 4H; H3, H3″), 8.31 (d, J = 8.5 Hz, 4H; H_{Ar}), 8.24−8.12 (12H; H_{Pery}, H4, H4″), 7.80 (d, J = 5.0 Hz, 4H; H6, H6″), 7.65 (d, J = 8.5 Hz, 4H; H_{Ar}), 7.44 + $CHCl_3$ (m, 4H; H5, H5″), 7.28 (m, 16H; H_{Ar}), 6.87 (m, 16H; H_{Ar}), 4.10 (t, J = 6.5

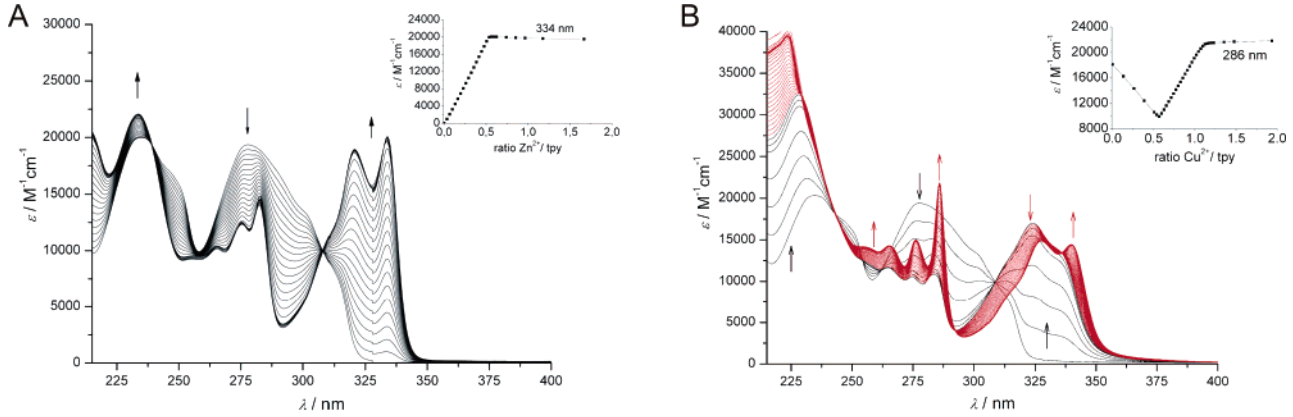

Figure 1. UV-vis titrations of tpy with (A) Zn^{2+} and (B) Cu^{2+} perchlorate hexahydrates in acetonitrile (0.5 mM tpy); black lines: < 0.5 equiv Cu^{2+}, red lines: > 0.5 equiv Cu^{2+}; insets show absorption changes at characteristic wavelengths.

Hz, 4H; NCH_2), 1.66 (m, 4H; CH_2), 1.41 (m, 4H; CH_2), 1.31 (s, 32H; CH_3), 1.29 (s, 32H; CH_3), 0.95 (t, J = 7.5 Hz, 6H; CH_3); UV−vis ($CHCl_3$): λ_{max} (ϵ) = 589 (103 500), 548 (60 700), 457 nm (34 000 $M^{-1}cm^{-1}$); fluorescence ($CHCl_3$): λ_{max} = 623 nm, quantum yield: Φ_{fl} = 0.90 ($CHCl_3$), 0.75 (DMF), lifetime (λ_{ex} = 520 nm, λ_{em} = 645 nm): τ = 6.3 ns ($CHCl_3$), 5.5 ns (DMF); MS (MALDI-TOF, DCTB[32]): *m/z* (%) 2904.05 (100) $[M - OTf]^+$, 2755.15 (10) $[M - 2OTf + H]^+$, 1554.52 (10) [**5a** + Zn + $OTf]^+$, 1345.59 (20) [**5a** + $H]^+$ (calcd for $C_{180}H_{158}F_6N_{10}O_{22}S_2Zn$: 3056.81).

Coordination Polymer 8a. To a solution of the ditopic ligand **3a** (19.6 mg, 12.3 μmol) in $CHCl_3$−CH_3CN (80:20, 4 mL) a stock solution of zinc triflate (10 mM, 1.23 mL, 12.3 μmol) was added and the solution was stirred for 1 h at room temperature. The exact 1:1 stoichiometry was checked by ^1H NMR and, if necessary, was adjusted until no residual signals of uncomplexed ligand was observed. The solution was concentrated, the product was precipitated by addition of more acetonitrile (10 mL) and isolated quantitatively by centrifugation. ^1H NMR (400 MHz, $CDCl_3/CD_3CN$ (80:20), TMS): δ = 9.03 (br, 4H; H3′), 8.75 (br, 4H), 8.4−8.1 (br, 8H), 7.82 (br, 4H), 7.66 (br, 4H), 7.43 (br, 4H, overlapped with $CHCl_3$ signal), 7.31 (br, 8H; H_{Ar}), 6.92 (br, 8H; H_{Ar}), 1.31 (br, 36 H; CH_3); UV−vis (DMF, ϵ value calculated per perylene unit): λ_{max} (ϵ) = 575 (45 500), 537 (28 600), 446 nm (14 750 M^{-1} cm^{-1}); fluorescence (DMF): λ_{max} = 613 nm, quantum yield (DMF): Φ_{fl} = 0.61, lifetime (DMF, λ_{ex} = 520 nm, λ_{em} = 645 nm): τ = 4.9 ns.

Results and Discussion

Studies on tpy Complexation. Because selection of a properly suited metal ion is crucial to obtain a long polymeric chain by reversible supramolecular polymerization of terpyridine-functionalized perylene bisimide building blocks, our first attention was directed to finding a suitable metal ion. Accordingly, the complexation of several first row transition metal ions with the parent terpyridine ligand was studied by UV−vis and ^1H NMR titration, as well as isothermal titration calorimetry (ITC). The metal(II) perchlorate hexahydrate salts of Fe^{2+}, Co^{2+}, Ni^{2+}, Cu^{2+}, and Zn^{2+} in acetonitrile were used as a consistent set of compounds. For all metal ions, distinct changes in tpy absorption was observed upon complexation and clear isosbestic points were found (Figure 1 and Figures S1−S3 in Supporting Information), indicating that only a single equilibrium between two species, namely free and complexed tpy, occurs during the titration. Whereas iron and cobalt complexes show intense absorption also in the visible region (λ > 400 nm) due to metal−ligand charge-transfer absorption, the complexes of Ni^{2+} and Cu^{2+} only absorb weakly in this area and the Zn^{2+} complex does not absorb at wavelengths higher than 350 nm (Figure 1A). Titration curves (Figure 1, insets) show a linear increase and a sharp endpoint at a metal/ligand ratio of 0.5:1, indicating the formation of a $M(tpy)_2^{2+}$ (2:1) complex. Due to the lack of curvature in the titration curve, no binding constants could be determined. Except for the Cu^{2+} complex (Figure 1B), no change of the UV−vis spectra could be observed when more than 0.5 equiv of metal were added to the solution. The addition of excess metal ion should cause the formation of a $M(tpy)^{2+}$ complex (1:1 complex) with solvent molecules or counterions as additional ligands for the case of reversible complexation. However, this reversibility cannot be assessed from UV−vis titrations as the changes in the spectra originate from the complexation of one tpy molecule with one metal ion, independent of the type of complex, i.e., $M(tpy)^{2+}$ or $M(tpy)_2^{2+}$ complex.

In contrast to all other metal ions used in this study, the respective titration with Cu^{2+} (Figure 1B) reveals an additional process. Up to a molar ratio of 0.5 (Figure 1B, black lines), the curve resembles the one shown in Figure 1A. However, a sharp change of the absorption spectrum at Cu^{2+}/tpy ratios > 0.5 were observed, indicating reversibility of the $Cu(tpy)_2^{2+}$ species (Figure 1B, red lines) and suggesting that the binding mode of the tpy units is different in $Cu(tpy)^{2+}$ and $Cu(tpy)_2^{2+}$ complexes.

Further insight into the structure of the complex species formed during the titration was obtained from ^1H NMR experiments, which were carried out using iron(II) and zinc(II) perchlorate hexahydrate salts in d_3-acetonitrile. Due to the perpendicular arrangement of the two aromatic tpy units in a $M(tpy)_2^{2+}$ complex, the tpy proton signals undergo pronounced changes as a result of magnetic shielding;[33] thus, the complexes $M(tpy)_2^{2+}$ and $M(tpy)^{2+}$ can be distinguished by ^1H NMR, which is not possible by UV−vis and ITC. In NMR studies, no dissociation was found for the $Fe(tpy)_2^{2+}$ complex even after addition of an excess amount of Fe^{2+}; rather, the signals of uncomplexed tpy ligand and the resulting $Fe(tpy)_2^{2+}$ complex were observed. This behavior points at a high kinetic barrier for the iron(II) complex. In contrast, titration of tpy solutions with both zinc perchlorate and zinc trifluoromethane sulfonate (triflate, OTf) led to a third set of signals after exceeding the ratio of 0.5, which can be attributed to the formation of a 1:1 complex of the type $Zn(tpy)^{2+}$ with acetonitrile molecules or the counterions as additional ligands (cf. Figure S4 in Supporting

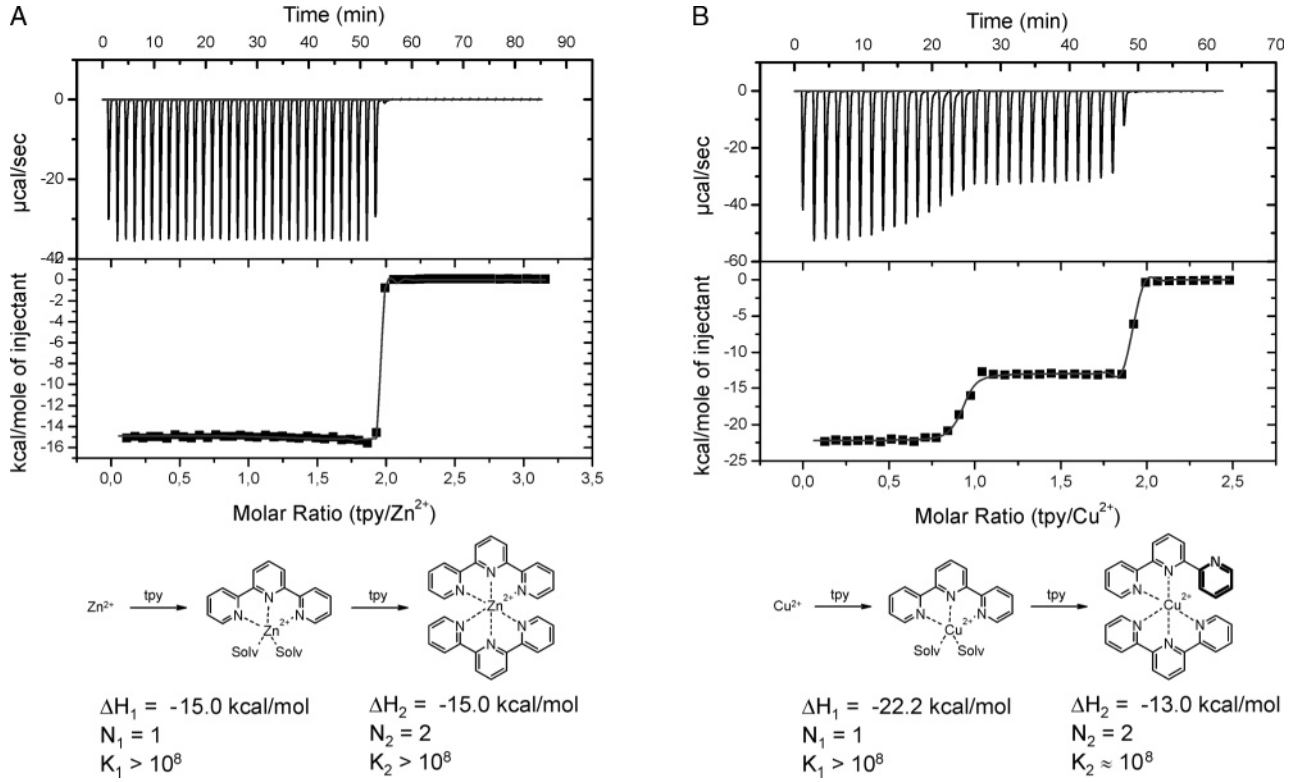

Figure 2. (A) ITC experiment with tpy and zinc(II) perchlorate hexahydrate in acetonitrile (0.5 mM). Experiments with Fe^{2+}, Co^{2+}, and Ni^{2+} provided similar titration curves only differing in absolute ΔH values; (B) titration with copper(II) perchlorate hexahydrate in acetonitrile (0.5 mM).

Information for the titration curve). These results also confirm fast exchange kinetics (reversibility). Although the coordination of Zn^{2+} to tpy is reversible, the exchange is slow on the NMR time scale; thus, separate proton NMR signals of the repective species were detected instead of averaged signals. Nevertheless, equilibrium has been reached within less than a minute.

The results obtained from our NMR experiments in acetonitrile are consistent with kinetic data determined by Hogg and Wilkins[34] for the reaction of various $M(tpy)_2$ complexes with excess tpy in water ($t_{1/2}$ for $Fe(tpy)_2^{2+}$, $Ni(tpy)_2^{2+}$, and $Co(tpy)_2^{2+}$ are 8400, 610, and 60 min respectively, compared to $t_{1/2} < 0.1$ min for the Zn^{2+} and Cu^{2+} complexes). The intermediate ligand exchange rate of $Co(tpy)_2^{2+}$ complexes has been investigated by Lehn et al.[35] and Constable et al.[36] by utilizing this for the construction of dynamic combinatorial libraries. Oxidation of the $Co(tpy)_2^{2+}$ to $Co(tpy)_2^{3+}$ fixed the combinatorial library since Co^{3+} undergoes nearly irreversible, i.e., kinetically inert, complexation with tpy. Schubert and co-workers[14] found from viscosimetry experiments with tpy-substituted poly(ethylene oxide) that Fe^{2+} and Ni^{2+} complexes are kinetically inert, whereas those of Co^{2+}, Cu^{2+}, and Cd^{2+} were found to be of labile nature.

Isothermal Titration Calorimetry (ITC) with Terpyridine Complexes. The advantage of ITC method for the determination of the complexation behavior is that the titration experiment can be monitored in both directions, i.e., addition of metal salt to tpy solution and vice versa. Thus, the heat of complexation can also be determined if tpy is added to a solution of the metal salt, a process which cannot be monitored by NMR or UV−vis spectroscopy. Figure 2A shows a typical ITC titration experiment with zinc perchlorate hexahydrate and tpy. As expected, the $Zn(tpy)_2^{2+}$ formation is completed at a 0.5 molar ratio of Zn^{2+}/tpy. This titration provides evidence that the transformation of the 2:1 complex to the 1:1 complex (the existence of the latter has been proven by ^1H NMR) does not give any calorimetric signal, indicating that the only process yielding reaction heat is the complexation of the free tpy unit with metal ion. Similar observation has been made for Fe^{2+}, Co^{2+}, Ni^{2+}, and Zn^{2+} with varying absolute ΔH values (Table 1). Cu^{2+} is the only system in this series to deviate from this behavior, as already observed by UV−vis titration. Figure 2B shows the ITC titration results of the copper(II) perchlorate hexahydrate/tpy system in acetonitrile. Two calorimetrically distinguished processes can be found for Cu(II) in clear contrast to the previously investigated metal ions. These observations suggest that in the case of $Cu(tpy)_2^{2+}$ only one tpy ligand acts as a tridentate ligand, whereas the second tpy is merely attached by two of the three pyridine units as known for 2,2′-bipyridine (bpy) complexes.[37]

For all titrations by ITC, the $\Delta H°$ values and the stoichiometries could be determined exactly due to clearly defined start and end values of the isotherm. For the same reason, it was not possible to derive exact

Table 1. Enthalpies and Lower Limits for the Binding Constants Determined for a Series of $M(tpy)_2(ClO_4)_2$ Complexes by ITC[a]

	$M^{2+} \rightarrow M(tpy)^{2+}$		$M(tpy)^{2+} \rightarrow M(tpy)_2^{2+}$	
	ΔH^0_1/kcal mol^{-1}	K_1/M^{-1}	ΔH^0_2/kcal mol^{-1}	K_2/M^{-1}
Fe^{2+}	−19.1	$>10^8$	−19.1	$>10^{10}$
Co^{2+}	−14.7	$>10^8$	−14.7	$>10^{10}$
Ni^{2+}	−16.0	$>10^8$	−16.0	$>10^{10}$
Cu^{2+}	−22.2	$>10^8$	−13.0	$\approx 10^8$
Zn^{2+}	−14.5	$>10^8$	−14.5	$>10^{10}$

[a] Errors are ± 0.5 kcal mol^{-1} for ΔH^0.

Scheme 1

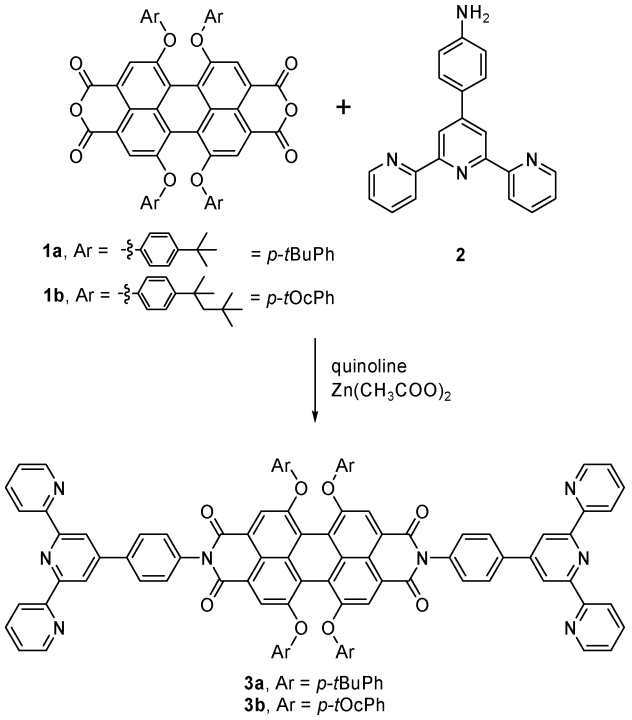

binding constants (or $\Delta G°$ values) and only a lower limit can be given (between $>10^8$ M^{-1} and $>10^{10}$ M^{-1}).

The data obtained from our titration experiments suggest that the tpy/Zn^{2+} interaction is very promising for the construction of high-molecular-weight luminescent coordination polymers from terpyridine-functionalized perylene bisimides. First, due to the closed-shell (d^{10}) electronic configuration of Zn^{2+}, no MLCT states arise upon coordination (UV−vis studies) which might quench the fluorescence of the perylene bisimide chromophore. Second, the pronounced ligand exchange rate of Zn^{2+}/tpy coordination ("reversibility") is favorable for the self-healing process in supramolecular self-assembly and offers the possibility for the formation of well-defined polymeric structures and their further organization in 2D and 3D solid-state materials (see AFM studies). Despite its reversible nature, the binding constant of $>10^8$ M^{-1} is pretty high compared to other noncovalent forces applied for supramolecular polymerization,[38] and therefore, the reaction of a ditopic tpy ligand with Zn^{2+} at a 1:1 stoichiometry is expected to lead to high-molecular-weight polymers even in dilute solution. Third, the octahedral coordination of Zn^{2+} ions will cause formation of rigid linear polymers of ditopic building blocks **3a,b** (in contrast to macrocyclization which often competes with supramolecular polymerization). Because of this unique combination of favorable properties, the supramolecular polymerization of tpy-equipped perylene bisimides **3** has been investigated with Zn^{2+} salts.

Synthesis. Ditopic terpyridine-functionalized perylene bisimide ligands **3a,b** were prepared by condensation of 4′-*p*-aminophenyl-2,2′:6′,2″-terpyridine (**2**) with the respective bisanhydrides **1a,b**[22,26] in quinoline with zinc acetate as catalyst in isolated yields of 37% (for **3a**) and 12% (for **3b**). As the monotopic ligands **5** are valuable model compounds for complexation studies, the condensation reaction of **2** was carried out with a mixture of the bisanhydride **1** and imide anhydride **4**, the latter is accessible via partial saponification of the corresponding

Chart 1

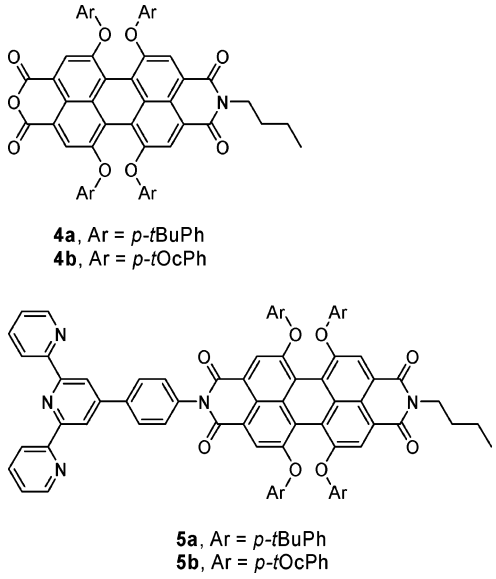

n-butyl bisimide.[24] The mixture of products **3** and **5** was separated by repetitive column chromatography on basic alumina of activity II. Due to strong adsorption of the tpy units to alumina, the isolated yields of the products are only moderate. Despite extended π systems, all compounds **3a,b** and **5a,b** exhibit good solubility in halogenated organic solvents due to the bulky phenoxy substituents bearing *tert*-butyl or 1,1,3,3-tetramethylbutyl (*tert*-octyl) groups.[20]

Dimer Complex Formation With Zinc Triflate. Complexation studies were first performed using the monotopic model compound **5**, which forms the dimer complex **6** upon addition of zinc triflate (Scheme 2). The solvent system for this complexation has to be well balanced to provide enough polarity to solubilize the metal salt and the ionic $[Zn(tpy)_2(OTf)_2]$ unit but still keep the extended aromatic system of the perylene bisimide in solution. Mixtures of chloroform−methanol were applied successfully in most complexation experiments, but in some cases, chloroform−acetonitrile (80/20) was the better choice.

The complexation reaction of monotopic ligands **5** with $Zn(OTf)_2$ was monitored by ^1H NMR. Figure 3 shows the characteristic ^1H NMR signals in the aromatic

Scheme 2

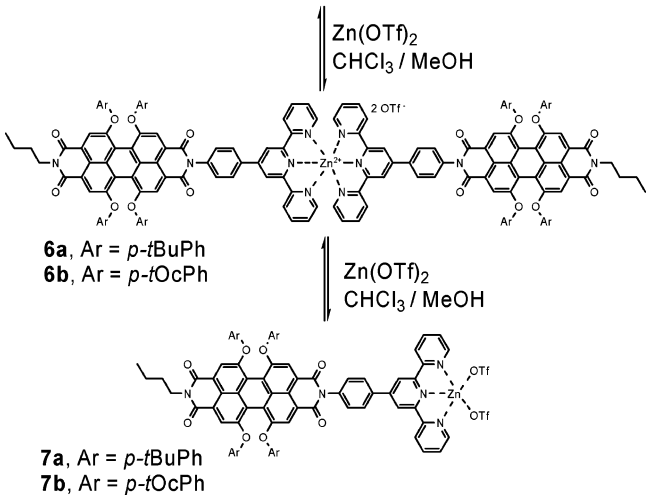

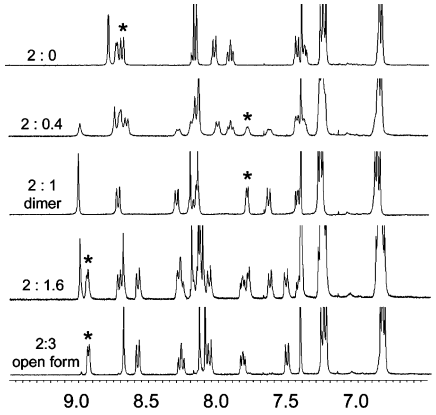

Figure 3. ^{1}H NMR spectra at different ligand/metal ion ratios for the monotopic ligand **5a** and zinc triflate in $CDCl_3-CD_3CN$ (80:20, 5 mM) from free **5a** (upper spectrum) to dimer **6a** (middle) and the opened form **7a** (bottom). The marked signal (*) corresponds to proton H6 adjacent to the lateral pyridine nitrogen atoms.

Scheme 3

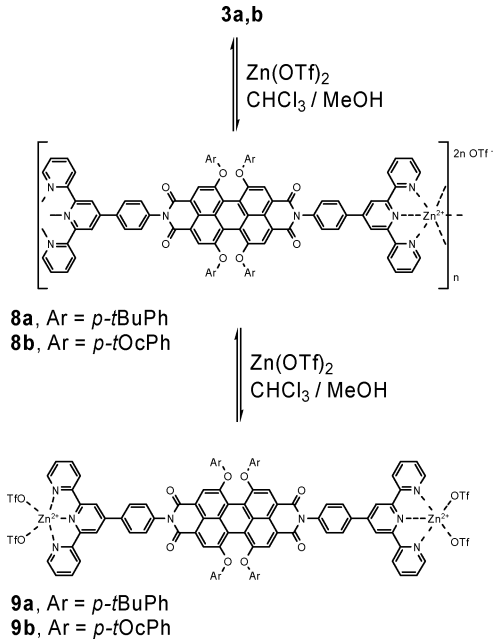

region during the titration at different ligand/metal ratios. The formation of dimer **6a** is clearly indicated by the disappearance of the original set of signals which belong to the uncomplexed ligand **5a** and the rise of a second set of signals, exemplified by the drastic high-field shift of protons H6,6″ at the outer pyridine units (marked with * in Figure 3) from 8.74 to 7.80 ppm, which is mainly due to the aromatic shielding effect of the neighboring second tpy unit. At a ratio of 2:1, only the dimer **6a** is present in solution and the ^{1}H NMR signals can be clearly assigned. Once this ratio is exceeded by addition of more Zn^{2+} ions, the dimer signals decrease in intensity again and a third set of signals evolves, demonstrating again reversible Zn^{2+}–terpyridine bonding. The new formed species may be assigned to a 1:1 complex **7a** with the additional coordination sites of the metal center saturated either by acetonitrile molecules or triflate counterions (see Scheme 3). Also here, as in the case of unsubstituted tpy, the exchange kinetics is slow on the NMR time scale, but equilibrium has been reached within a few seconds after addition of zinc triflate. Despite its lability,

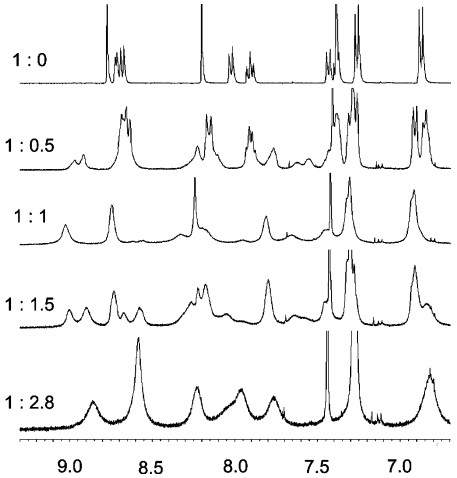

Figure 4. ^{1}H NMR spectra at different ligand/metal ion ratios for the ditopic ligand **3a** and zinc triflate in $CDCl_3-CD_3CN$ (80:20; concentrated of **3a**: 5 mM) from free **3a** (upper spectrum) to polymer **8a** (middle, 1:1) and the fragmented dicomplexed form **9a** (bottom).

dimer **6a** could be characterized by MALDI-TOF mass spectrometry revealing the mass of the dimer cation with one triflate counterion (Supporting Information, Figure S5).

Polymer Formation from Ditopic Ligands 3a,b with Zinc Triflate. In analogy to dimer complex formation of monotopic ligand **5**, ditopic ligand **3a,b** should afford extended coordination polymers when mixed with exactly 1 equiv of Zn^{2+}. To confirm the formation of coordination polymers, a similar titration as in the case of ligand **5** was performed with the ditopic ligand **3a**. As can be seen from Figure 4, the ^{1}H NMR titration resembles the situation observed for the formation of complex **6**, and the characteristic proton chemical shifts of different species are observed in the same regions. The formation of a coordination polymer can be concluded from the following observations: Upon addition of zinc triflate, broadening is observed for the first upcoming set of signals, which becomes the only set of signals present in the spectrum when 1:1 stoichiometry is reached. As the solution remains clear and no precipitation or further aggregation can be observed, this signal broadening can be attributed to the formation of coordination polymer **8a**. Comparison of the ^{1}H NMR spectra of polymer **8a** (Figure 4, 1:1) and the model dimer **6a** (Figure 3, 2:1) shows the identical set of signals, but in the former case, they are significantly broadened. Again, reversible complexation is observed when excess Zn^{2+} is added to the coordination polymer solution, which results in the shortening of the polymer strands to form a distribution of oligomeric and monomeric fragments such as **9a** with two monocomplexed Zn^{2+} units at the ends.

The polymer length at a 1:1 ratio can be estimated from the ^{1}H NMR signals of the end groups to a minimum of 10 repeat units corresponding to a chain length of 30 nm and a minimum molecular weight of ~16 600 g/mol. Since the coordination polymer is of $(A-B)_n$ type, its chain length depends critically on realization of an exact 1:1 stoichiometry, and even small deviations cause a drastic decrease in polymer length.[22] This fact, together with the very hygroscopic nature of the zinc triflate is the reason that all coordination compounds have not been prepared in a classical synthetic manner but by a titration method using ^{1}H

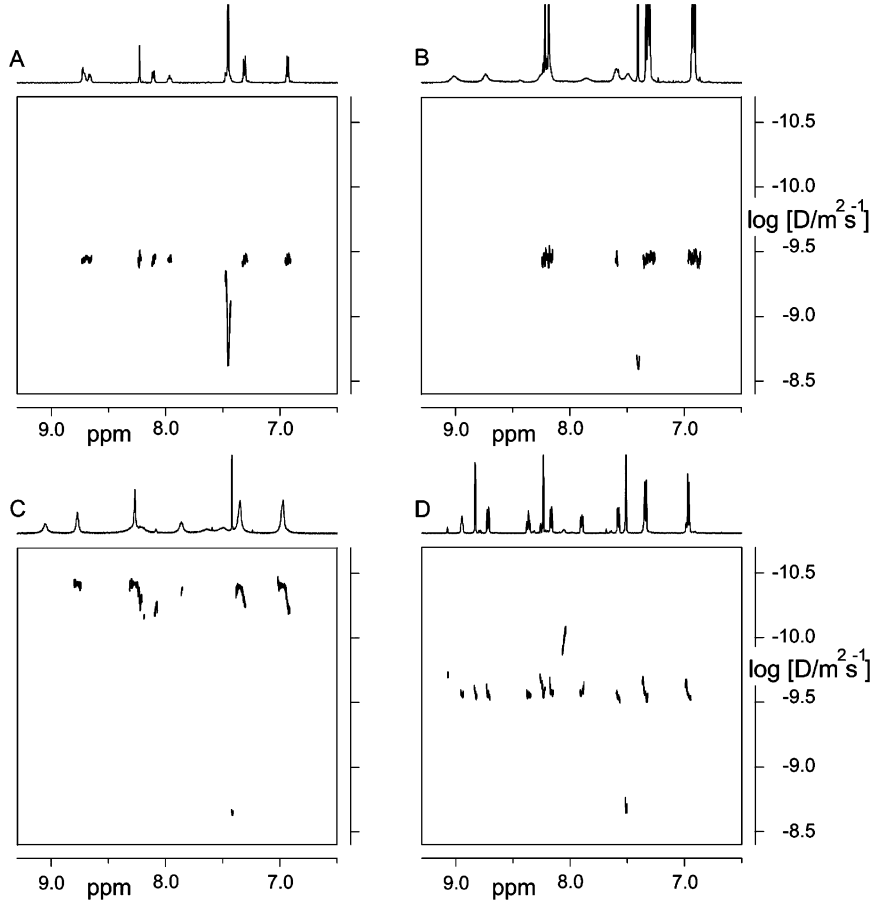

Figure 5. Aromatic region of the ^{1}H DOSY NMR spectra of monomer **3b** (A), dimer **6b** (B), polymer **8b** (C), and the fragmented species **9b** (D) in chloroform−methanol (80:20; concentration 2.5 mM). The diffusion coefficients, D (in m^2/s), are plotted in a logarithmic scale against the chemical shift, δ.

NMR to ensure the precise 1:1 stoichiometry. Despite several attempts, mass spectrometric characterization of the coordination polymers by MALDI-TOF MS was not successful, as only fragments showing the ligand with one Zn^{2+} ion could be observed due to fragmentation during the ionization process.

Although the initial solubility of both coordination polymers **8a,b** is good in chloroform/methanol, as well as chloroform/acetonitrile mixtures, differences are observed for long-term solubility. Whereas polymer **8a** with the *tert*-butylphenoxy residues at the perylene bisimide core slowly starts to precipitate within 1 day after preparation, polymer **8b** is solubilized sufficiently by the bulky *tert*-octylphenoxy residues to form stable, clear solutions for weeks. Both coordination polymers are also highly soluble over long periods of time in DMF, and ^{1}H NMR spectra recorded in deuterated *N*,*N*-dimethylformamide (DMF) reveal that the coordination remains unchanged. Several attempts have been made to assess the polymer length by gel permeation chromatography (GPC), but using different solvents under varying conditions, only the signal corresponding to the molecular mass of the monomer has been found. This observation can be explained in terms of the reversible nature of the complex bond. Due to the nonequilibrium conditions during a GPC run, the constant dilution and shear forces might cause fragmentation of the coordination polymers. A further explanation for the exclusive detection of monomers may be that the charged polymer chains adsorb to the stationary phase.

DOSY NMR Studies. To further substantiate the formation of oligomeric and polymeric species, ^{1}H DOSY (diffusion ordered spectroscopy)[39] NMR experiments were carried out. This two-dimensional NMR technique correlates the ^{1}H NMR signals with the diffusion coefficient of the respective species in solution and has recently been successfully introduced for the characterization of supramolecular coordination polymers.[40,41] The DOSY spectra were recorded in chloroform−methanol (80:20) first for the monomeric ligand **3b** alone, then after addition of 1 equiv of Zn^{2+} providing coordination polymer **8b**, and subsequently after addition of 2 equiv more of Zn^{2+}, which should lead to fragmentation of polymer **8b** to low-molecular-weight species such as **9b**. Figure 5 shows the aromatic region of the DOSY NMR spectra for monomer **3b** (A), polymer **8b** (C), and fragments (D) with the corresponding ^{1}H NMR spectrum plotted against the logarithm of the diffusion coefficient. As the monomer **3b** is itself a large molecule with a molecular weight of $M = 1822$ g/mol, it appears at a significantly smaller diffusion coefficient ($\log D = -9.45$) in comparison to the chloroform molecule ($\log D = -8.66$). The diffusion coefficient of the coordination polymer **8b** is in the range of $\log D = -10.45$, 1 order of magnitude smaller than that of the monomer **3b**. The strong decrease of diffusion coefficient upon addition of one equivalent of Zn^{2+} ion to monomer **3b** clearly indicates the formation of an extended, high-molecular-weight polymer structure with the corresponding ^{1}H NMR signals characteristic for the complexed form of the tpy unit. Upon addition of more than 1 equiv of Zn^{2+} to monomer **3b**, the diffusion coefficient increases to a value in the range of $\log D = -9.5$ to -9.7, which is slightly smaller than that of the monomer,

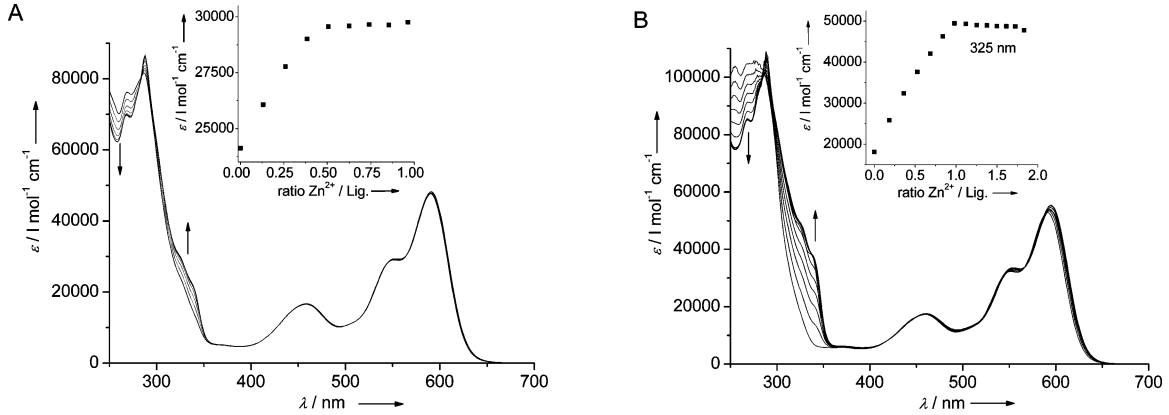

Figure 6. Spectral changes upon addition of zinc triflate to monotopic (A, **5a**) and ditopic (B, **3a**) perylene bisimide ligands in $CHCl_3$–MeOH (60:40); insets show apparent absorption coefficient (at 325 nm) as a function of the Zn^{2+}/ligand ratio.

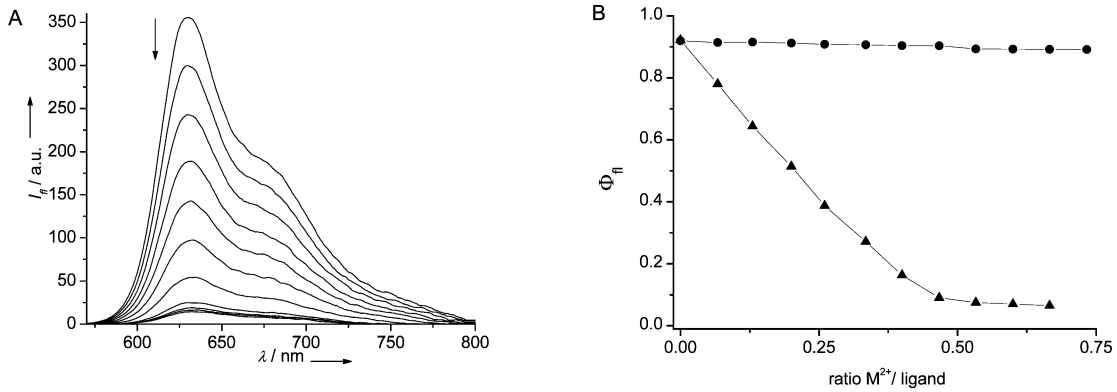

Figure 7. Fluorescence quenching (A) of monotopic perylene bisimide ligand **5a** by addition of iron(II) perchlorate hexahydrate and fluorescence quantum yields (B) as a function of iron(II)/**5a** ratio (triangles) and zinc(II)/**5a** ratio (circles). All measurements in $CHCl_3$–MeOH (60:40), 10^{-5} M.

indicating fragmentation of the coordination polymer to low-molecular-weight oligomers. For comparison, also the DOSY result of the dimer model compound **6b** is depicted in Figure 5B. The diffusion coefficient of the model complex, which exhibits nearly twice the volume of the uncomplexed ditopic ligand **3b**, is virtually identical to that of ligand **3b**. This indicates that a significantly larger number of units is necessary to cause a 10-fold decreased diffusion coefficient as found for the polymer **8b**.

UV–Vis Absorption Properties. All uncomplexed monotopic (**5a,b**) and ditopic (**3a,b**) ligands show the characteristic absorption bands of the tetraphenoxy-substituted perylene bisimide chromophore between 500 and 650 nm ($S_0 \rightarrow S_1$, $\epsilon = 50\,000$–$55\,000$ L mol^{-1} cm^{-1}) and 400–500 nm ($S_0 \rightarrow S_2$), whereas at wavelengths below 350 nm, both the perylene bisimide and the terpyridine units absorb. UV–vis titration experiments of the monotopic and ditopic building blocks were performed to assess the ground state interaction of the perylene bisimide chromophore with the terpyridine unit; the latter should act purely as the structure determining part. Figure 6 shows the UV–vis titration of the mono- and ditopic *tert*-butylphenoxy-substituted ligands **5a** and **3a** with zinc triflate. As expected from the studies with the parent terpyridine ligand, complexation does not have any significant influence on the absorption of the perylene bisimide chromophore. However, an increase in absorbance between 300 and 350 nm and a decrease at wavelengths below 300 nm was observed, corresponding to the change in tpy absorption (cf. Figure 1A). These changes can be assigned to the complexation of the tpy unit which fixes the three pyridine units in an all-cis conformation. The dimeric compex of **5a** does not show any significant change in the perylene bisimide absorption band compared to the uncomplexed form (see Figure 6A), while the polymer exhibits a small increase in the absorption coefficient and a small red-shift of the absorption maximum from 591 to 594 nm.

Fluorescence Properties. All tpy-substituted perylene bisimide compounds exhibit intense red fluorescence ($\lambda_{max} = 620$ nm) with fluorescence quantum yields around $\Phi_{fl} = 0.9$ in halogenated solvents such as chloroform or dichloromethane. The effect of metal complexation on the fluorescence properties of the perylene bisimide fluorophore unit was investigated by steady-state fluorescence spectroscopy. Figure 7A depicts the fluorescence titration of monotopic perylene ligand **5a** with both zinc(II) triflate and iron(II) perchlorate hexahydrate. The fluorescence of **5a** is drastically quenched upon addition of Fe^{2+} ions (Figure 7A), which is in accord with the observed decrease of the fluorescence quantum yield from >0.9 for the uncomplexed ligand **5a** to <0.1 for the iron(II) complex (Figure 7B, triangles). In contrast, complexation with zinc(II) (Figure 7B, circles) has virtually no effect on the fluorescence quantum yield of perylene bisimide unit. The fluorescence quantum yields in DMF are reduced by ~20% independent of that, whether the perylene bisimide ligand is complexed or free (Table 2, compare **6a** and **3a**). This moderate reduction of quantum yield is apparently due to the solvent polarity. Likewise, fluorescence lifetimes are almost identical for uncomplexed ligand, dimer complex, and polymer species. These results imply that no electronic interactions take

Table 2. Emission Properties of Uncomplexed Ligands and Zn^{2+} Complexes[a]

	$CHCl_3$		DMF	
	Φ_{fl}	τ/ns	Φ_{fl}	τ/ns
monotopic ligand **5a**	0.89	–	–	–
dimer **6a**	0.90	6.3	0.74	5.5
ditopic ligand **3a**	0.92	6.1	0.75	4.8
polymer **8a**	–	–	0.61	4.9

[a] Errors for quantum yields are ±0.04, errors for lifetimes are ±0.2 ns except for **8a**: ±0.4 ns.

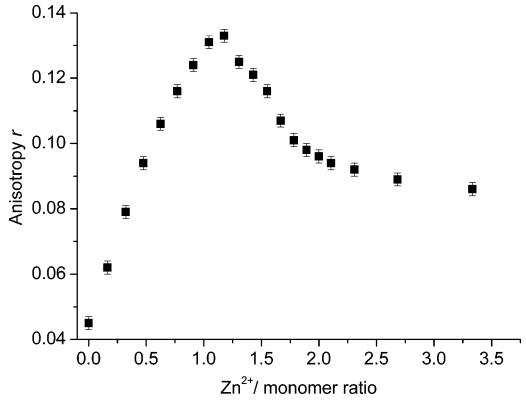

Figure 8. Fluorescence anisotropy titration of monomer **3b** with zinc triflate in chloroform−methanol (60:40, [**3b**] = 2.5×10^{-5} M, λ_{ex} = 550 nm, λ_{em} = 610 nm, 20.0 ± 0.05 °C), error bars are ±0.005.

place between $Zn(tpy)_2$ coordination sites and the perylene bisimide unit.

Fluorescence Anisotropy Titration. The significant change in size and shape of the species upon addition of Zn^{2+} ions into a solution of perylene bisimide ligands due to the formation of coordination polymer from monomer and fragmentation of polymer to oligomers on addition of excess Zn^{2+} has pronounced effect on the diffusion properties (^{1}H DOSY NMR experiments). With the intense fluorescence of the coordination polymer **8a,b** another method to obtain structural and photophysical information becomes available, i.e., fluorescence anisotropy measurements. The values of fluorescence anisotropy, r, can range from −0.2 to +0.4. In solvents of low viscosity at room temperature, the anisotropy is decreased by rotational diffusion, making it suitable to study changes in size of fluorescent systems. The maximum value can be reached in the absence of rotational diffusion and other depolarization effects, such as energy transfer, and if a parallel orientation of the absorption and emission transition dipole moments is given.[42]

Figure 8 shows a plot of the fluorescence anisotropy, r, of the perylene ligand **3b** against the Zn^{2+}/**3b** ratio. The chromophore was excited in the S_0-S_1 transition at 550 nm, and the fluorescence was detected at 610 nm to ensure the highest possible anisotropy value. The titration was performed in a chloroform−methanol mixture to ensure comparability with the UV−vis and fluorescence titration experiments. For the monomer **3b**, an anisotropy value of r = 0.045 was observed which increased nearly linearly to a maximum of r = 0.133 at a 1:1 ratio of Zn^{2+}/**3b**. These results are in accordance with the formation of coordination polymer since significantly slower rotational diffusion of polymer lead to higher anisotropy because of its enlarged size. Due to the fact that in the rigid coordination polymer all chromophores are aligned in the direction of their fluorescence transition dipole moments, which are located along the N−N axis of the perylene bisimide unit, potential energy transfer within the perylene bisimide units along the strands will not decrease anisotropy. As expected, the anisotropy decreases again upon exceeding the 1:1 stoichiometry due to the fragmentation of the polymer into oligomeric units. The value saturates at r = 0.091, indicating that these fragments are significantly smaller than the polymer but still larger than the monomeric unit. These results are consistent with that of the DOSY NMR experiments. A similar titration experiment with ligand **3a** showed the same characteristics, only differing in the absolute r values, which were r = 0.048 for the monomer, r = 0.096 for the polymer (**8a**), and r = 0.062 for the oligomeric fragments (at Zn^{2+}/monomer ratios > 1.7). The smaller values for **8a** may be explained in terms of the sterically less demanding *tert*-butyl groups compared to the very bulky *tert*-octyl residues in **8b**. The smaller steric demand lowers the molecular volume of **8a** and, consequently, increases the diffusion coefficient.

Atomic Force Microscopy (AFM) of the Coordination Polymers. The aim of atomic force microscopy experiments was to determine the shape and length of the single polymer strands, as well as their two-dimensional organization on a surface. The uncomplexed ligand molecules **3a**, which were deposited via spin-coating of DMF solution onto freshly cleaved mica, appeared as isolated dots (Figure 9A). The height of these globular objects was found to be quite homogeneous with a mean value of 1.6 ± 0.1 nm. Due to the tip broadening effect, a rather high value of 9.2 ± 1.2 nm was obtained for the mean diameter of the particles. Samples of the coordination polymers **8a,b** were prepared by spin-coating of DMF solutions of different concentration on both mica and HOPG (highly ordered pyrolytic graphite) substrates. AFM images of the polymers **8a,b** (Figure 9B, F−H) clearly show the fibrous appearance of the polymers on both types of substrates. Mean heights of the strands reveal the same value of 1.6 ± 0.1 nm for both polymers **8a,b**. However, in comparison to the very uniform heights, the apparent length of the rods shows a broad distribution. For both polymers, long filaments up to 400 nm in length, as well as very small globular objects, similar to the ligand molecules, can be observed. The apparent length of the polymers measured by AFM revealed a mean value of 50.1 ± 5.3 nm. Molecular modeling of the ligand and the coordination polymer (Figure 10) reveals a length of 3 nm for each repeat unit. Comparison of the measured mean length with the calculated model suggests that a single rod is formed from approximately 15 repeat units corresponding to a molecular weight of ~25 000. The diameter of the polymer strand determined from molecular modeling is 1−2 nm and depends on the conformation of the phenoxy residues. This is in very good agreement with the measured height of 1.6 nm, suggesting that no lateral aggregation of the strands takes place. Other information which can be extracted from molecular modeling studies is the relative flexibility of the polymer strand. Although the $M(tpy)_2$ unit facilitates a very rigid linkage, the two single bonds of the phenyl rings connecting perylene bisimide and tpy provide some flexibility which has also been found in AFM micrographs.

Investigation of the polymer samples prepared using solutions of higher concentration (1 mM) reveals the

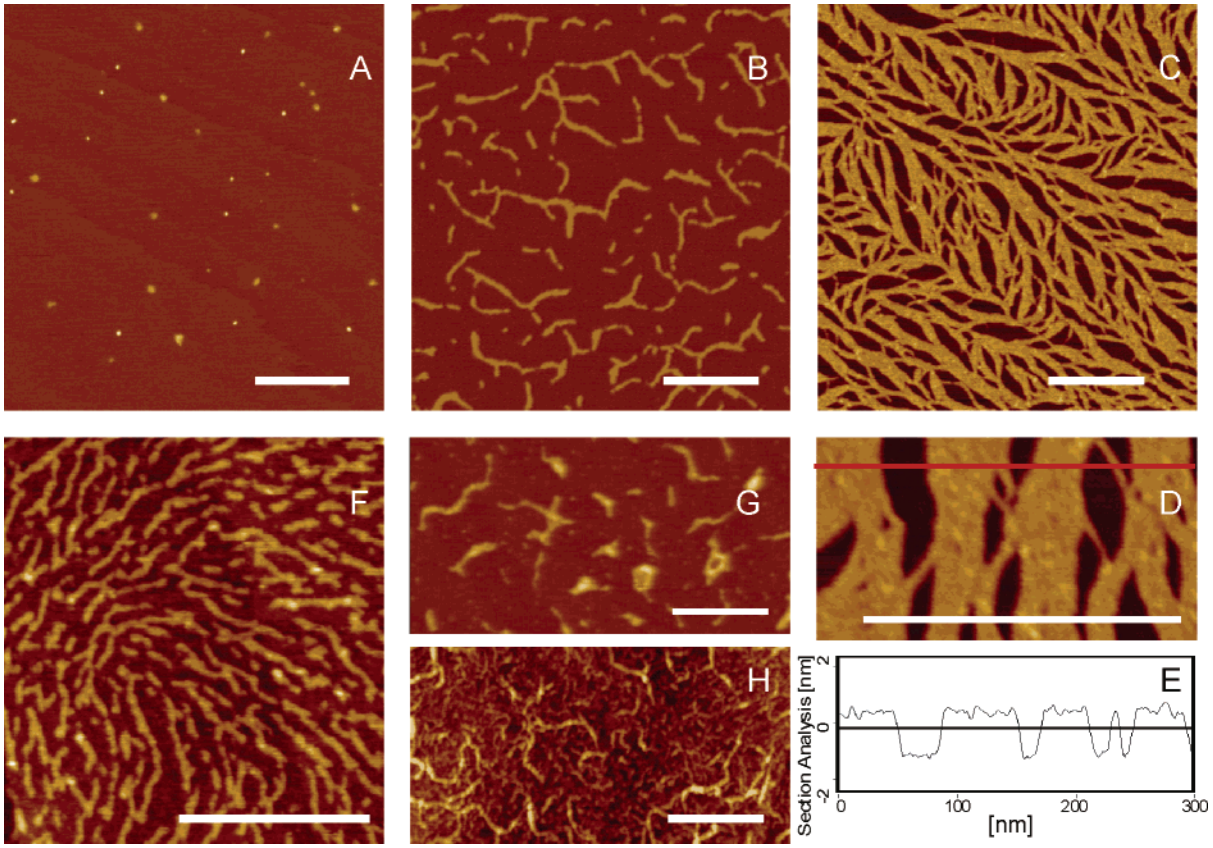

Figure 9. (A) AFM image of ligand **3a** on mica and the corresponding coordination polymer **8a** prepared from dilute (B, 0.1 mM) and concentrated (C, 1 mM) DMF solution on mica; (D) high-resolution AFM image with assembled polymeric chains. A cross-section along the red line is presented in (E); (F) coordination polymer **8a** (0.1 mM) on HOPG; coordination polymer **8b** (0.05 mM) on mica (G) and HOPG (H). In all AFM images, the scale bar corresponds to 250 nm, the *z* data scale is 5 nm. All samples were prepared by spin-coating.

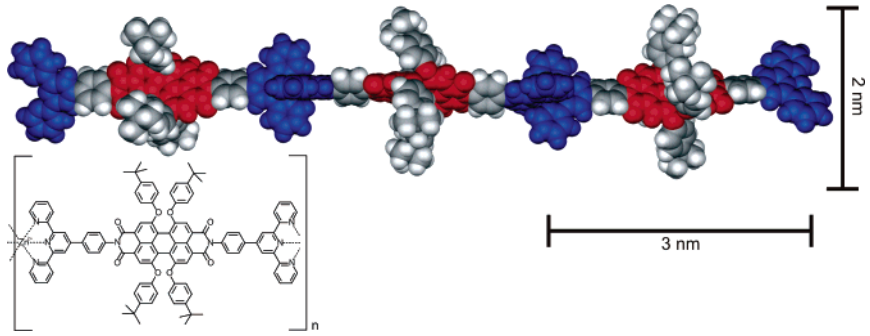

Figure 10. Molecular modeling (Fujitsu Quantum CAChe 5.2, MM3 force field) and schematic representation of coordination polymer **8a**; three repeat units are shown, perylene bisimide units are represented in red, $Zn(tpy)_2$ units in blue.

formation of a monolayer over large areas in the micrometer range for both types of substrates (Figure 9C and D). Also in this case, analysis of the apparent height measured from the AFM images revealed a constant value of 1.5 ± 0.1 nm (Figure 9D, E). From the AFM images, it is evident that the neighboring strands tend to interact with each other, leading to two-dimensional self-assembly. Because of the spreading of the polymer samples in the surface plane, probably caused by the spin-coating process, defects in the cylinders' packing are observed, enabling the visualization of single rods. Lateral dimensions of the single rods were measured to be approximately 4 nm. Definitely, at higher concentration, the polymer tends to aggregate by contacting terminally and laterally to form a network of closely packed rods. As the surface of freshly cleaved mica bears negative charge, the interaction with the coordination polymer, being a polycation, is expected to be very strong, which explains the uniform coverage with a monolayer film. Formation of such monolayers is highly desirable for any kind of (opto)electronic device. As shown by our study, it seems possible to achieve well-ordered 2D monolayers from metallosupramolecular 1D polymeric chains formed in solution. Notably, such polymeric structures of ionic compounds cannot be realized by vacuum sublimation techniques.

Conclusion

Starting with studies on the complexation behavior of 2,2′:6′,2″-terpyridine with first row transition metal ions and the characterization of the thermodynamically stable (high binding constant) but kinetically labile (fast ligand exchange) coordination of Zn^{2+} ions, metallo-supramolecular self-assembly of functional perylene

bisimide dyes to polymeric structures has been realized. Perylene bisimide chromophores were equipped with tpy ligands by condensation of the respective anhydrides with 4′-*p*-aminophenyl-2,2′:6′,2″-terpyridine (**2**) to form monotopic (**5a,b**) and ditopic (**3a,b**) building blocks. The complex formation was investigated by the preparation of a dimer complex (**6a,b**) using two monotopic units. On the basis of these results, highly soluble coordination polymers (**8a,b**) have been prepared from Zn^{2+} complexation of ditopic building blocks. For both dimer and polymer, reversible coordination was observed depending on the ratio of Zn^{2+}/ligand, resulting for the polymer in a drastically decreased chain length when the Zn^{2+}/ligand ratio exceeds 1:1. Fluorescence properties of the coordination compounds are excellent with high fluorescence quantum yields also for the polymeric compounds. The hypothesis of reversible self-assembly and de-assembly of a high-molecular-weight coordination polymer at Zn^{2+} excess was supported by the results of DOSY NMR and fluorescence anisotropy measurements. Both methods are sensitive to the diffusion coefficients of the analyte and resulted in a significantly decreased diffusion coefficient for the polymer compound in comparison to the ligand and the fragments obtained by exceeding 1:1 ratio. Visualization of the coordination polymer was possible by AFM microscopy, and the average chain length was determined to 15 units, which is in agreement with the value of >10 units obtained from ^{1}H NMR. AFM also revealed the formation of a surprisingly homogeneous monolayer on negatively charged substrates. This observation and preliminary results for further hierarchical structure formation[43] using the multilayer assembly technique introduced by Decher[44] render this self-assembled functional system as an interesting alternative to traditional main chain perylene bisimide polymers[26] for application in artificial light harvesting systems or organic light emitting diode fabrication.

Acknowledgment. Financial support by the Deutsche Forschungsgemeinschaft (DFG grant project WU 317/3-1), and DAAD "Acciones Integradas Hispano-Alemanas" is gratefully acknowledged. We are thankful to Shimadzu Germany for the measurement of the MALDI-TOF MS of compound **6a**. The authors also thank L. De Cola, M. Rehahn, and R. Ziessel for helpful discussions on terpyridine metal complexes and H. Kessler and B. Luy for their help with the DOSY NMR technique.

Supporting Information Available: Experimental details for DOSY NMR, fluorescence anisotropy, ITC, and AFM measurements. Details for ^{1}H NMR, UV−vis, and fluorescence titration experiments. Spectra of UV−vis titrations of tpy with Fe^{2+}, Co^{2+}, and Ni^{2+} and a ^{1}H NMR titration plot of tpy with Zn^{2+}. This material is available free of charge via the Internet at http://pubs.acs.org.

References and Notes

(1) Friend, R. H. *Pure Appl. Chem.* **2001**, *73*, 425−430 and references therein.
(2) Brabec, C. J.; Saricifci, N. S.; Hummelen, J. C. *Adv. Funct. Mater.* **2001**, *11*, 15−26.
(3) Mitschke, U.; Bäuerle, P. *J. Mater. Chem.* **2000**, *10*, 1471−1507.
(4) Archer, R. D. *Coord. Chem. Rev.* **1993**, *93*, 49−68.
(5) Rehahn, M. *Acta Polym.* **1998**, *49*, 201−224.
(6) Manners, I. *Science* **2001**, *294*, 1664−1666.
(7) Constable, E. C.; Cargill Thompson, A. M. W. *J. Chem. Soc., Dalton Trans.* **1992**, 3467−3475.
(8) Sauvage, J.-P.; Collin, J.-P.; Chambron, J.-C.; Guillerez, S.; Coudret, C.; Balzani, V.; Barigelletti, F.; De Cola, L.; Flamigni, L. *Chem. Rev.* **1994**, *94*, 993−1019.
(9) Barigelletti, F.; Flamigni, L. *Chem. Soc. Rev.* **2000**, *29*, 1−12.
(10) Ziessel, R.; Hissler, M.; El-Ghayoury, A.; Harriman, A. *Coord. Chem. Rev.* **1998**, *178−180*, 1251−1298.
(11) Newkome, G. R.; He, E.; Moorefield, C. N. *Chem. Rev.* **1999**, *99*, 1689−1746.
(12) Kelch, S.; Rehahn, M. *Macromolecules* **1999**, *32*, 5818−5828.
(13) Schütte, M.; Kurth, D. G.; Linford, M. R.; Cölfen, H.; Möhwald, H. *Angew. Chem., Int. Ed.* **1998**, *37*, 2891−2893.
(14) Schmatloch, S.; van den Berg, A. M. J.; Alexeev, A. S.; Hofmeier, H.; Schubert, U. S. *Macromolecules* **2003**, *36*, 9943−9949.
(15) Michelsen, U.; Hunter, C. A. *Angew. Chem., Int. Ed.* **2000**, *39*, 764−767.
(16) Ogawa, K.; Kobuke, Y. *Angew. Chem., Int. Ed.* **2000**, *39*, 4070−4073
(17) El-Ghayoury, A.; Schenning, A. P. H. J.; Meijer, E. W. *J. Polym. Sci. A: Polym. Chem.* **2002**, *40*, 4020−4023.
(18) Yu, S.-C.; Kwok, C.-C.; Chan, W. K.; Che, C.-M. *Adv. Mater.* **2003**, *15*, 1643−1647.
(19) Beck, J. B.; Rowan, S. J. *J. Am. Chem. Soc.* **2003**, *46*, 13922−13923.
(20) Würthner, F. *Chem. Commun.* **2004**, 1564−1579.
(21) Würthner, F.; Thalacker, C.; Diele, S.; Tschierske, C. *Chem. Eur. J.* **2001**, *7*, 2245−2253.
(22) Würthner, F.; Thalacker, C.; Sautter, A.; Schärtl, W.; Ibach, W.; Hollricher, O. *Chem. Eur. J.* **2000**, *6*, 3871−3886.
(23) Thalacker, C.; Würthner, F. *Adv. Funct. Mater.* **2002**, *12*, 209−218.
(24) Würthner, F.; Sautter, A.; Schmid, D.; Weber, P. J. A. *Chem. Eur. J.* **2001**, *7*, 894−902.
(25) You, C.-C.; Würthner, F. *J. Am. Chem. Soc.* **2003**, *125*, 9716−9725.
(26) (a) Dotcheva, D.; Klapper, M.; Müllen, K. *Macromol. Chem. Phys.* **1994**, *195*, 1905−1911. (b) Thelakkat, M.; Posch, P.; Schmidt, H.-W. *Macromolecules* **2001**, *34*, 7441−7447.
(27) A part of this paper was published as a communication: Dobrawa, R.; Würthner, F. *Chem. Commun.* **2002**, 1878−1879.
(28) Perrin, D. D.; Armarego, W. L. F. *Purification of Laboratory Chemicals*, 2nd ed.; Pergamon Press: Oxford, 1980.
(29) Mukkala, V.-M.; Helenius, M.; Hemmilae, I.; Kankare, J.; Takalo, H. *Helv. Chim. Acta* **1993**, *76*, 1361−1378.
(30) Lakowicz, J. R. *Principles of Fluorescence Spectroscopy*, 2nd ed.; Kluwer Academic/Plenum: New York, 1999.
(31) Gvishi, R.; Reisfeld, R.; Burshtein, Z. *Chem. Phys. Lett.* **1993**, *213*, 338−344.
(32) MALDI-MS Matrixes: dithranol = 1,8,9-anthracenetriol, DHB = 2,5-dihydroxybenzoic acid, DCTB = *trans*-2-(3−4-*tert*-butylphenyl)-2-methyl-2-propenylidene)malonitrile
(33) Thummel, R. P.; Jahng, Y. *Inorg. Chem.* **1986**, *25*, 2527−2534.
(34) Hogg, R.; Wilkins, R. G. *J. Chem. Soc.* **1962**, 341−350.
(35) Goral, V.; Nelen, M. I.; Eliseev, A. V.; Lehn, J.-M. *Proc. Natl. Acad. Sci.* **2001**, *98*, 1347−1352.
(36) Constable, E. C.; Housecroft, C. E.; Kulke, T.; Lazzarini, C.; Schofield, E. R.; Zimmermann, Y. *J. Chem. Soc., Dalton Trans.* **2001**, 2864−2871.
(37) Priimov, G. U.; Moore, P.; Helm, L.; Merbach, A. E. *Inorg. React. Mech.* **2001**, *3*, 1−23.
(38) Brunsveld, L.; Folmer, B. J. B.; Meijer, E. W.; Sijbesma, R. P. *Chem. Rev.* **2001**, *101*, 4071−4097.
(39) Johnson, C. S., Jr. *Prog. NMR Spectrosc.* **1999**, *34*, 203−256.
(40) Paulusse, J. M. J.; Sijbesma, R. P. *Chem. Commun.* **2003**, 1494−1495.
(41) Vermonden, T.; van der Gucht, J.; de Waard, P.; Marcelis, A. T. M.; Besseling, N. A. M.; Sudhölter, E. J. R.; Fleer, G. J.; Cohen Stuart, M. A. *Macromolecules* **2003**, *36*, 7035−7044.
(42) Haas, U.; Thalacker, C.; Adams, J.; Fuhrmann, J.; Riethmüller, S.; Beginn, U.; Ziener, U.; Möller, M.; Dobrawa, R.; Würthner, F. *J. Mater. Chem.* **2003**, *13*, 767−772.
(43) Dobrawa, R.; Kurth, D. G.; Würthner, F. *Polym. Prepr.* **2004**, *45*, 378−379.
(44) Decher, G. *Science* **1997**, *277*, 1232−1237.

MA047737J